Crystal Engineering

Deutsche Ausgabe: DOI: 10.1002/ange.201606003
Internationale Ausgabe: DOI: 10.1002/anie.201606003

Self-Healing Molecular Crystals

*Patrick Commins, Hideyuki Hara, and Panče Naumov**

Abstract: *One of the most inevitable limitations of any material that is exposed to mechanical impact is that they are inexorably prone to mechanical damage, such as cracking, denting, gouging, or wearing. To confront this challenge, the field of polymers has developed materials that are capable of autonomous self-healing and recover their macroscopic integrity similar to biological organisms. However, the study of this phenomenon has mostly remained within the soft materials community and has not been explored by solid-state organic chemists. The first evidence of self-healing in a molecular crystal is now presented using crystals of dipyrazolethiuram disulfide. The crystals were mildly compressed and the degree of healing was found to be 6.7 %. These findings show that the self-healing properties can be extended beyond mesophasic materials and applied towards the realm of ordered solid-state compounds.*

The deterioration and accumulation of damage of materials over time has been a commonly accepted maxim by people for thousands of years. The discovery of the self-healing materials has begun to challenge this idea by creating materials that are able to autonomously repair themselves after a mechanical defect has been introduced.[1–4] The field gained its breakthrough in 2001 when White and co-workers reported the first autonomously self-healing polymer,[5] and it has been growing exponentially over the past 15 years.[6–8] Self-healing polymers and composites have been created using microencapsulated healing agents,[9] thermal reactions,[10] supramolecular interactions,[11–13] and other mechanisms.[14–16] However, the interest in this exciting area of research has remained limited to the soft materials research community and it has not been explored by solid-state chemists, mainly because of the perceived rigidity, slow diffusion, and chemical inertness of solids. However, recent advancements in solid-state chemistry[17–23] have been aimed towards dispelling these beliefs and, considering that the migration of mass across the surface of molecular crystals can be substantial[24–26] we presume the self-healing concept can be extended to ordered molecular solids. Herein, we describe the findings towards the first evidence of self-healing in a molecular crystal.

[*] Dr. P. Commins, Prof. P. Naumov
New York University Abu Dhabi,
Abu Dhabi (United Arab Emirates)
E-mail: pance.naumov@nyu.edu
Dr. H. Hara
Bruker Biospin K.K.
3–9, Moriya, Kanagawa, Yokohama, Kanagawa 221-0022 (Japan)
Supporting information and the ORCID identification number(s) for the author(s) of this article can be found under: http://dx.doi.org/10.1002/anie.201606003.

Having polymers as a source of inspiration, the design of a self-healing crystal required the selection of a chemically reactive reaction system that would be applicable to molecular crystals. Microencapsulate[27] and nanoparticle-based polymers[28] and other multicomponent materials were omitted because they cannot be realized with molecular crystals. Other self-healing polymers that are based on Diels–Alder cycloadditions[29] or ligand-exchange reactions[30] were also not applicable since they would require introduction of supramolecular templates.[31] Instead, we drew ideas from dynamic covalent chemistry, which utilizes molecules that undergo rapid reversible bond formations.[32,33] From dynamic molecular systems with identical reacting species, disulfides were ultimately selected based on the low bond dissociation energy and reversibility of the bond reformation close to ambient conditions.[34–37] With this in mind, we decided to study dipyrazolethiuram disulfide (1*H*-pyrazole-1-carbothioic dithioperoxyanhydride) **1** (Figure 1). The ease of homolytic dissociation of the disulfide bond in **1** and the delocalization of the ensuing radicals across the two sulfur atoms should allow the resulting radical to readily regenerate the disulfide bridge with a nearby reactive neighbor. Additionally, radical-shuffling-based self-healing polymers have been proven to be quite robust and some can heal without external stimuli.[38–40]

Compound **1** was synthesized in one step using an adapted procedure from a previous report[41] (Supporting Information, Scheme S1). A shallow non-penetrating incision was manually applied along the *a* axis on the {010} face of a pristine single crystal (Figure 1 A and B; defecting a face was necessary as the defect guided the propagation of the fracture). The crystal was then flipped over and adhered to silicone pads, which were glued to a tensile tester. The crystal was then cracked along its *a* axis by applying local pressure (Figure 1 C), and the two halves were separated (Figure 1 D and E). The bifurcated pieces were compressed under 1–3 N of force and maintained at rest at room temperature, under ambient light for 24 h (Figure 1 F). After decompression, the strength of adhesion between the pieces was analyzed. The self-healing process was later repeated without adhering the crystals to the pads or adhering the pads to the tester. The crystals were considered healed if could be lifted from one edge and support their own weight across the crack. The healed crystals were not only able to resist minor forces such as gravity (Figure 1 G and H; Supporting Information, Movie S1), but also gentle poking with a polyamide tip (Figure 1 I and J). While some of the crystals separated under this stress, quite remarkably, others did not.

The percent healing is calculated by measuring the tensile strength of the virgin material against the healed material.[6,7] The tensile strength of **1** was acquired by pulling a pristine crystal apart (Figure 2 A–D). As the sample is pulled the line shape shows a gradual increase in the load due to the elastic

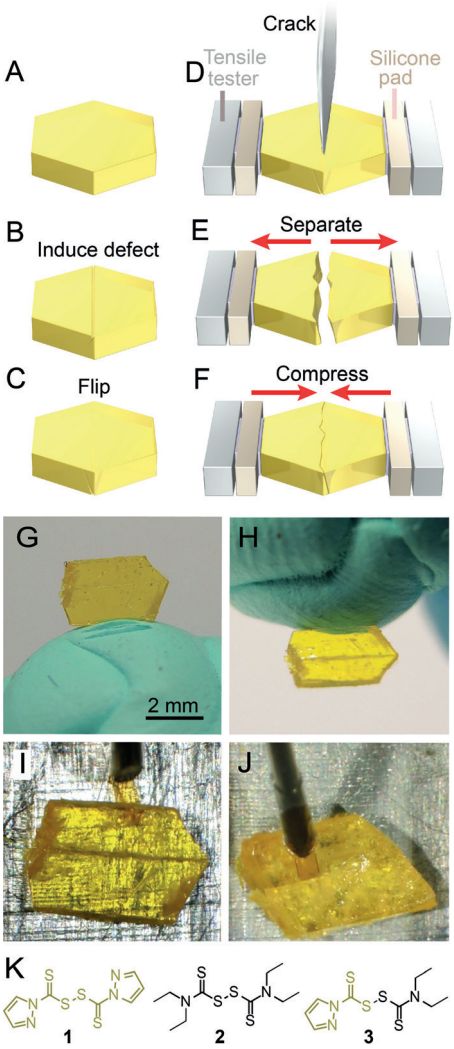

Figure 1. The procedure for cracking and healing a crystal of **1**. A),B) A shallow non-penetrating incision is made along the *a* axis on the {010} face of the crystal by using a scalpel. C) The crystal is then flipped and adhered onto the tensile tester. D) The crystal is cracked by applying localized pressure. E),F) The two pieces are completely separated, compressed and left to self-heal for 24 hours. G) An optical image of a healed crystal of **1** mounted in putty. H) The same crystal is then inverted. I),J) A healed crystal did not separate after being lifted from the cracked side or even after being poked by a polyamide tip. K) Chemical structures of compounds **1**, **2**, and **3**.

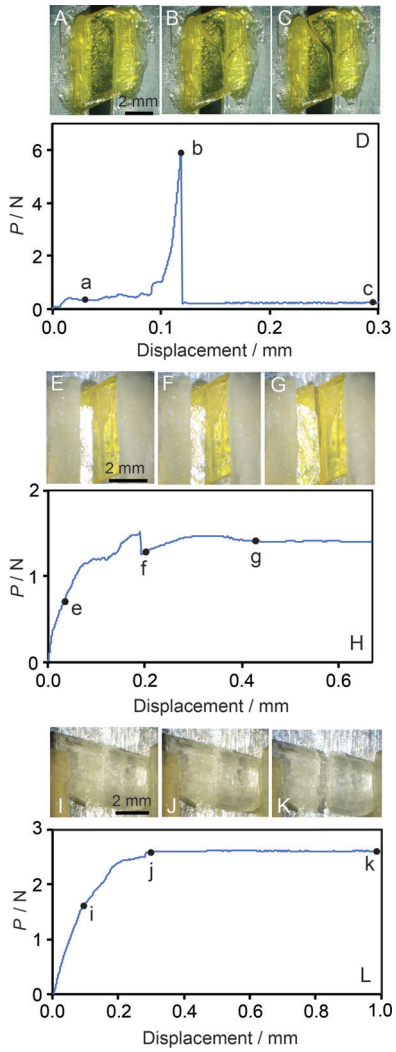

Figure 2. Mechanical evidence of self-healing crystal. A)–D) Images and tensile strength profile of a pristine crystal of **1**. E)–H) Images and tensile strength of a self-healed crystal of **1**. The sharp decrease in load before point f corresponds to separation of the adhered pieces. The calculated healing versus the virgin material is 6.7%. I)–L) Images and tensile strength profile of tetraethylthiuram disulfide (**2**), a crystal that is not able to self-heal.

component of the glue–crystal interface. The sample reaches a point of fracture (Figure 2B), followed by a steep drop and flattening of the curve after separation (Figure 2C). The average load decrease at the separation point normalized by the cross-sectional area between the two faces of two crystals gives a tensile strength of 1.1 MPa. The tensile profile of a healed crystal is displayed in Figure 2D–G. At a displacement of 0.03 mm (point e in Figure 2H), the crystal is still compressed by the pads and there is a rapid increase in force as they are decompressed. After a displacement of 0.18 mm (Figure 2F), the crystal–crystal interface becomes strained and breaks, as shown by the sudden drop in load at 0.19 mm (point f in Figure 2H). Based on the drop in the force normalized to the surface area, the healed crystal had a tensile strength of 0.086 MPa, which corresponds to 7.8% healing. The average tensile strength of two healed crystals was 0.074 MPa, which gives a healing of 6.7%.

Inspection by SEM revealed the topographic details of the healed crystal (Figure 3A–D). While the front face of the crystal is well faceted (Figure 3C), relatively smooth, and the appearance of the crack is not apparent, the kerf created by the scalpel blade can be seen running across the middle of the back face (Figure 3D). The zoomed-in images of the interface between the two parts in Figure 3E and F show areas where the two pieces are still separated. However, there are also areas of attachment where the pieces are physically connected (Supporting Information, Comment 1).

The topology of the healed crystals was further inspected using confocal fluorescence microscopy. The fluorescence

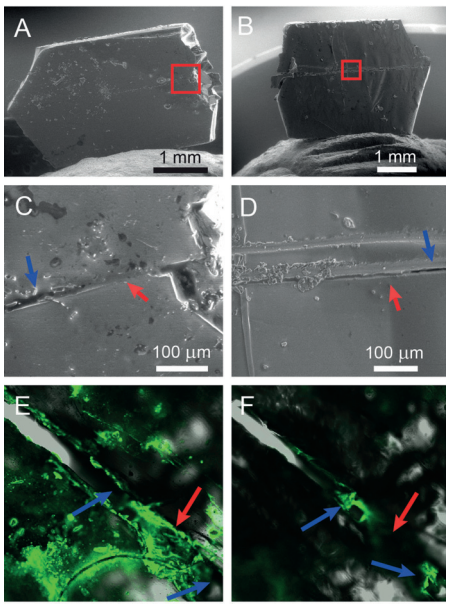

Figure 3. Imaging of healed crystals of **1**. A),B) SEM image of the front and back face of the healed crystal. C),D) Zoomed-in images of the highlighted sections in (A) and (B). Blue and red arrows highlight areas of separation and attachment, respectively. E) A healed crystal coated with a fluorescent dye was imaged using confocal fluorescence microscopy and the material spanning the cracked region (red arrow) is fluorescent. F) The dye is found at both sides of the attached region running along the walls signifying the disconnected areas (blue arrows).

images overlaid against the optical images of a partially healed crystal at two different depths are shown in Figure 3 E and F, and a movie with the 3D scan is available in the Supporting Information, Movie S2. All of the exposed surfaces of the crystal were coated with the dye, and the area of attachment between the two halves was also fluorescent. When the crystal is imaged at a lower depth the disconnected portions come into focus. The dye runs along the walls of these areas of separation from the top to the bottom. However, the attached areas only show fluorescence at the surface of the crystal, and the dye was not found at other focal depths. These images provide qualitative evidence that the two pieces are connected.

Because the SEM was unable to acquire information on the internal structure of the crystal, we turned to X-ray computed tomography (CT) to visualize the internal features of the healed crystal by probing the spatially resolved density using X-ray absorption (Figure 5; Supporting Information, Movies S3 and S4). The facets, angles, and features from the electron and optical micrographs are reproduced in the CT images, and the crack is visible as a light green line running across the center of the crystal. The crack between the two sides of the crystal can also clearly be seen by the bright green line between the two pieces on the far left side in the cross-sectional

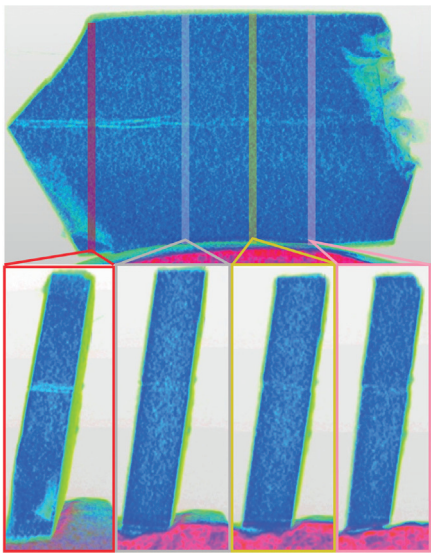

Figure 4. A CT scan of the healed crystal. The cross-sections are presented below the image, showing the disappearance of the crack.

analysis (highlighted by the red bar in Figure 4). As the scan proceeds along the long axis of the crystal the green coloration from the crack begins to dissipate and a much more homogenous blue color appears, indicating uniform density across the sample (see the cross-sectional images in Figure 4). The homogeneity of the blue coloration across the entirety of the crystal substantiates the attachment of the two pieces in the crystal interior. Furthermore, the color gradient in the region of the crack indicates that there is a change in density along the recess, in support of the concept according to which there are areas where the crystal is separated, partially healed, and fully healed.

We postulated that the self-healing is caused by shuffling of S–S bonds across the cracked interfaces. In the crystal, the S–S bond would homolytically break and the radical would be delocalized across the two sulfur atoms. The radical could then interact with a nearby sulfur atom, forming a new S–S bond, and the reaction would propagate (Figure 5). To substantiate the possibility of disulfide shuffling, mixed

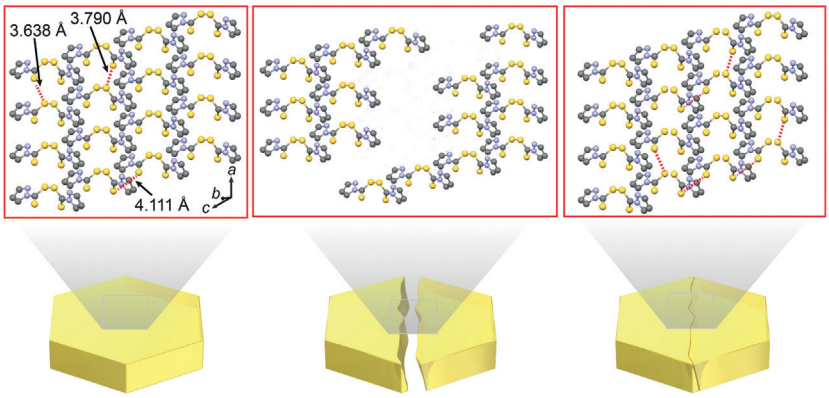

Figure 5. Crystal structure and the postulated mechanism of healing. During the compression the radicals are able to shuffle and bond to nearby molecules, whereby the two pieces are rejoined. The S–S distances are rounded; hydrogen atoms were omitted for clarity.

solutions of **1** and the tetraethylthiuram disulfide **2** (Supporting Information, Figure S1) in [D_6]benzene were studied using ^{1}H NMR spectroscopy (Supporting Information, Figure S2). In principle, the two compounds should be able to shuffle, and if equimolar solutions of **1** and **2** are mixed, a 1:2:1 mixture of **1**, **3**, and **2** will form, as shown previously.[37] Not surprisingly, after 24 hours of mixing, the peak of the heterodimer ethylpyrazolethiuram disulfide (**3**) begins to appear as a small shoulder at 8.06 ppm in the ^{1}H NMR spectrum. As time progresses, the intensity of the peak from **3** increases and the peak at 7.98 ppm decreases. After 149 hours, the reaction has progressed to a 1:1:1 ratio. The slow reaction progression in solution can be rationalized by the ESR spectra (described below), which show the R–S$^{\bullet}$ radical signal is below the limit of detection in solutions of benzene; thus, it is reasonable to assume the reaction may proceed slower than previously reported.[37] However, the reaction proceeds in solution and it can occur at ambient conditions and under visible light. We assume this reaction is equally possible in the solid and the disulfide bonds between adjacent molecules can shuffle and reform to heal the two halves of the crystal.

Previous ESR measurements on similar thiuram disulfides have shown that an air-stable radical is present in the solid and in solution.[42,43] Once the radicals are generated, whether by mechanical force, heat, or light irradiation, they are expected to be able to propagate within the crystalline lattice. Past research in this field performed by the McBride's group has demonstrated propagation of radical chain reactions throughout molecular layers.[44] Both solids and solutions of **1** were studied by ESR spectroscopy (Supporting Information, Figure S3). At 298 K, in the dark, solution of **1** shows a signal at $g = 2.004$. When the sample is irradiated with visible light, an additional signal at $g = 2.009$ is observed, and when irradiated with UV light, a third signal occurs at $g = 2.024$. When a crystalline powder is used, an identical spectrum is obtained regardless of irradiation, and the three signals ($g = 2.004$, 2.009, and 2.026) are present. This result confirms that the radical species necessary for shuffling are present at ambient temperature and even without irradiation (Supporting Information, Comment 2).[45]

The shuffling mechanism requires proximity of the S–S bonds in the crystal. The X-ray crystal structure of **1**[46] shows there are three prominent sulfur–sulfur contacts of 3.6375(8), 3.7898(7), and 4.1107(8) Å (Figure 5). The 3.6375(8) and 3.7898(7) Å contacts appears to be ideal for shuffling, as the atoms are perfectly positioned to form a new bond. However, experimentally the split crystal cannot be easily compressed along this axis because of its rhombohedral morphology; it has two sloped sides of 114° and when the pieces are compressed, they slide and eventually slip. Indeed, the crystal could only be compressed along the sides that were flat, which required splitting along the *a* axis. Along the *c* axis there is a close contact between two sulfur atoms of 4.1107(8) Å. This interaction should be able to create new covalent bonds between the two cracked halves and may be responsible for the healing (Supporting Information, Comment 3). A degree of S–S bond shuffling may also occur between the two sulfur atoms along the *a* axis of the crystal (Figure 5), but it is less clear whether this contributes to the healing. To assess the possibility of pressure-induced transition, the phase of the solid was investigated by powder XRD after successive grinding durations, and no phase transitions were observed (Supporting Information, Figure S4).

The shuffling of the disulfide bonds across the contact surface would require significant mass transport at the interface. To study the molecular migration at the crystal surface of **1**, the {010} face was indented with a diamond-tipped AFM cantilever. The resulting canyon and pileup features were monitored using AFM (Figure 6; Supporting Information, Movie S5). After 7.5 hours, the pileup features have noticeably decreased in height. After 62.5 hours almost all of the features have dissipated and only the initial indent is visible. Each of the peaks decreases fairly linearly with respect to time but at different rates (Supporting Information, Figure S6). This observation can be rationalized by the peak morphology; wider, more blunt features are expected to decrease slower than sharp, narrow peaks. For instance, peak 1 (Supporting Information, Figure S5, blue line) with initial height of 0.49 μm slowly recedes into the baseline features after 37 hours. The average rate of decrease of the three features was 9.4 nm h^{-1}. Assuming that this rate is indicative of the mass transfer at the surface, it implies that when the sample is compressed for 24 hours, the material may move up to 225 nm during the compression time to achieve contact and heal.

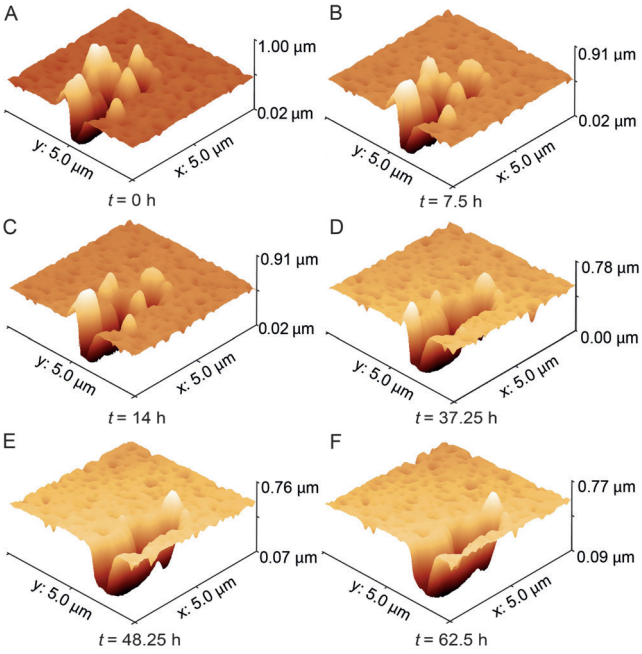

Figure 6. Mass transport at the surface of the crystal of **1** observed by AFM. The images of the indented sample over 62.5 h. The pileup features gradually disappear over time, indicating significant mass transfer.

In conclusion, we have obtained evidence for the first example of a self-healing organic molecular crystal. The crystals exhibit about 6.7 % healing at ambient conditions,

with no other external stimuli other than moderate mechanical compression. We postulate the disulfide shuffling mechanism is responsible for the self-healing property. The crystal structure of **1** contains three different S–S contacts that are proximal and they may be capable of forming new bonds. The radicals proposed for the shuffling mechanism are also observed, and a degree of mass transfer necessary to span the interstitial gaps in between the two interfaces was also found. We believe other molecular crystals may also be capable of this phenomenon.

Acknowledgements

The experiments were partially carried out using Core Technology Platform resources at NYU Abu Dhabi. We thank Dr. James Weston for assistance with the CT and Dr. Gijo Raj for help with the AFM.

Keywords: computed tomography · crystal engineering · disulfides · self-healing · smart materials

How to cite: *Angew. Chem. Int. Ed.* **2016**, *55*, 13028–13032
Angew. Chem. **2016**, *128*, 13222–13226

[1] C. Edvardsen, *ACI Mater. J.* **1999**, *96*, 448–454.
[2] H. M. Jonkers, A. Thijssen, G. Muyzer, O. Copuroglu, E. Schlangen, *Ecol. Eng.* **2010**, *36*, 230–235.
[3] H. J. Yang, Y. T. Pei, J. C. Rao, J. T. M. De Hosson, *J. Mater. Chem.* **2012**, *22*, 8304–8313.
[4] G. Q. Xu, M. J. Demkowicz, *Phys. Rev. Lett.* **2013**, *111*, 145501.
[5] S. R. White, N. R. Sottos, P. H. Geubelle, J. S. Moore, M. R. Kessler, E. N. Brown, S. Viswanathan, *Nature* **2001**, *409*, 794–797.
[6] D. Y. Wu, S. Meure, D. Solomon, *Prog. Polym. Sci.* **2008**, *33*, 479–522.
[7] E. B. Murphy, F. Wudl, *Prog. Polym. Sci.* **2010**, *35*, 223–251.
[8] Y. Yang, M. W. Urban, *Chem. Soc. Rev.* **2013**, *42*, 7446–7467.
[9] E. N. Brown, S. R. White, N. R. Sottos, *J. Mater. Sci.* **2004**, *39*, 1703–1710.
[10] X. Chen, M. A. Dam, K. Ono, A. Mal, H. Shen, S. R. Nutt, K. Sheran, F. Wudl, *Science* **2002**, *295*, 1698–1702.
[11] A. Phadke, C. Zhang, B. Arman, C. C. Hsu, R. A. Mashelkar, A. K. Lele, M. J. Tauber, G. Arya, S. Varghese, *Proc. Natl. Acad. Sci. USA* **2012**, *109*, 4383–4388.
[12] I. Jeon, J. Cui, W. R. K. Illeperuma, J. Aizenberg, J. J. Vlassak, *Adv. Mater.* **2016**, *28*, 4678–4683.
[13] Q. Wang, J. L. Mynar, M. Yoshida, E. Lee, M. Lee, K. Okuro, K. Kinbara, T. Aida, *Nature* **2010**, *463*, 339–343.
[14] B. Ghosh, M. W. Urban, *Science* **2009**, *323*, 1458.
[15] P. Cordier, F. Tournilhac, C. Soulié-Ziakovic, L. Leibler, *Nature* **2008**, *451*, 977–980.
[16] J. J. Cash, T. Kubo, A. P. Bapat, B. S. Sumerlin, *Macromolecules* **2015**, *48*, 2098–2106.
[17] P. Naumov, S. Chizhik, M. K. Panda, N. K. Nath, E. Boldyreva, *Chem. Rev.* **2015**, *115*, 12440–12490.
[18] C. S. Vogelsberg, M. A. Garcia-Garibay, *Chem. Soc. Rev.* **2012**, *41*, 1892–1910.
[19] S. Q. Su, T. Kamachi, Z.-S. Yao, Y.-G. Huang, Y. Shiota, K. Yoshizawa, N. Azuma, Y. Miyazaki, M. Nakano, G. Murata, S. Takeda, S. Kang, S. Kanegawa, O. Sato, *Nat. Commun.* **2015**, *6*, 8810.
[20] J.-K. Sun, W. Li, C. Chen, C. X. Ren, D. M. Pan, J. Zhang, *Angew. Chem. Int. Ed.* **2013**, *52*, 6653–6657; *Angew. Chem.* **2013**, *125*, 6785–6789.
[21] A. G. Shtukenberg, Y. O. Punin, A. Gujral, B. Kahr, *Angew. Chem. Int. Ed.* **2014**, *53*, 672–699; *Angew. Chem.* **2014**, *126*, 686–715.
[22] M. K. Panda, S. Ghosh, N. Yasuda, T. Moriwaki, G. D. Mukherjee, C. M. Reddy, P. Naumov, *Nat. Chem.* **2015**, *7*, 65–72.
[23] S. Hayashi, T. Koizumi, *Angew. Chem. Int. Ed.* **2016**, *55*, 2701–2704; *Angew. Chem.* **2016**, *128*, 2751–2754.
[24] G. Kaupp, M. R. Naimi-Jamal, *CrystEngComm* **2005**, *7*, 402–410.
[25] S. Varughese, M. S. R. N. Kiran, U. Ramamurty, G. R. Desiraju, *Angew. Chem. Int. Ed.* **2013**, *52*, 2701–2712; *Angew. Chem.* **2013**, *125*, 2765–2777.
[26] S. Varughese, M. S. R. N. Kiran, U. Ramamurty, G. R. Desiraju, *Chem. Asian J.* **2012**, *7*, 2118–2125.
[27] R. S. Trask, G. J. Williams, I. P. Bond, *J. R. Soc. Interface* **2007**, *4*, 363–371.
[28] J. Y. Lee, G. A. Buxton, A. C. Balazs, *J. Chem. Phys.* **2004**, *121*, 5531–5540.
[29] Y. Zhang, A. A. Broekhuis, F. Picchioni, *Macromolecules* **2009**, *42*, 1906–1912.
[30] Y. Shi, M. Wang, C. Ma, Y. Wang, X. Li, G. Yu, *Nano Lett.* **2015**, *15*, 6276–6281.
[31] T. Friščić, L. R. MacGillivray, *Chem. Commun.* **2003**, 1306–1307.
[32] Y. Jin, C. Yu, R. J. Denman, W. Zhang, *Chem. Soc. Rev.* **2013**, *42*, 6634–6654.
[33] A. Herrmann, *Chem. Soc. Rev.* **2014**, *43*, 1899–1933.
[34] R. Steudel, Y. Steudel, A. M. Mak, M. W. Wong, *J. Org. Chem.* **2006**, *71*, 9302–9311.
[35] M. M. Coleman, J. R. Shelton, J. L. Koenig, *Macromolecules* **2011**, *44*, 2536–2541.
[36] J. Canadell, H. Goossens, B. Klumperman, *Macromolecules* **2012**, *45*, 142–149.
[37] Y. Amamoto, H. Otsuka, A. Takahara, K. Matyjaszewski, *Adv. Mater.* **2012**, *24*, 3975–3980.
[38] K. Imato, M. Nishihara, T. Kanehara, Y. Amamoto, A. Takahara, H. Otsuka, *Angew. Chem. Int. Ed.* **2012**, *51*, 1138–1142; *Angew. Chem.* **2012**, *124*, 1164–1168.
[39] C. E. Yuan, M. Z. Rong, M. Q. Zhang, Z. P. Zhang, Y. C. Yuan, *Chem. Mater.* **2011**, *23*, 5076–5081.
[40] Y. Amamoto, J. Kamada, H. Otsuka, A. Takahara, K. Matyjaszewski, *Angew. Chem. Int. Ed.* **2011**, *50*, 1660–1663; *Angew. Chem.* **2011**, *123*, 1698–1701.
[41] L. N. Sobenina, A. P. Demenev, A. I. Mikhaleva, V. N. Elokhina, A. G. Mal'kina, O. A. Tarasova, I. A. Ushakov, B. A. Trofimov, *Synthesis* **2001**, 293–299.
[42] P. J. Nichols, M. W. Grant, *Aust. J. Chem.* **1983**, *36*, 1379–1386.
[43] M. Coleman, J. R. Shelton, J. L. Koenig, *Rubber Chem. Technol.* **1973**, *46*, 957–980.
[44] K. L. Pate, J. M. McBride, *Helv. Chim. Acta* **2000**, *83*, 2352–2362.
[45] O. Ito, K. Nogami, M. Matsuda, *J. Phys. Chem.* **1981**, *85*, 1365–1368.
[46] F. K. Keter, M. J. Nell, I. A. Guzei, B. Omondi, J. Darkwa, *J. Chem. Res.* **2009**, 322–325.

Received: June 21, 2016
Published online: September 16, 2016

